Boundary Burr Phenomenon for Long-path Time Domain OCT

Tatsuo Shiina [a]

Graduate School of Engineering, Chiba University, 1-33 Yayoi-cho, Inage-ku, Chiba-shi, Chiba 263-8522, Japan

Keywords: OCT, Long Path, Boundary, Diffraction.

Abstract: Long-path OCT measurement system has been developed for industrial use. We aim to measure time change of the concentration and refractive index of the target solution with a certain volume. As the fundamental experiment, we put the glass plate in the solution to obtain the glass position and its thickness, and got the interesting result. That is, the vibration mitigating waveform like a diffraction pattern by a knife-edge was observed. The OCT measurement consists of inline signals from the back-reflected (scattered) light, the diffraction pattern by a knife-edge is appeared on a screen. Although this phenomenon causes the boundary burr on the target detection, while the diffraction pattern has the information of the refractive index difference of the target. In this study, the characteristics of the boundary burr phenomenon is examined. Its origin is considered experimentally and analytically.

1 INTRODUCTION

The optical coherence tomography: OCT technology is the low coherent interferometer and it obtains the cross-sectional image by non-invasive and non-destructive measurement. It is invented by Tanno and Fujimoto (Tanno N., 1990 and Huang D., 1991) Mainly it is developed for ophthalmology (Danielson 1991, Brezinski, 1999) After that, it is adapted to the industrial use.(Song 2012) The combination of super luminescent diode: SLD and optical fiber interferometer adds the flexibility of measurement to the device and also compactness.

In this study, a portable OCT scanner has been developed for industrial use.(Shiina T., 2003, 2009, 2014, Yoshizawa T., 2015, Saeki K., 2020) The long path TD-OCT was aimed to measure the refractive index difference due to the solution condition such as temperature and density change or convective flow. The system has a measurement range of up to 100mm with 5-digit accuracy. And the target is not a drop of liquid, but a certain volume of the solution to catch the partial change in a volume and its temporal change. Long optical path measurement leads the sensitive detection to enlarge the small difference.

Recently, we conducted the fundamental experiment to evaluate the refractive index change due to the solution temperature (Shiina T. 2019) and

the aqueous solution of the ethanol was examined too with the unique characteristics of its refractive index variation. To expand the measurement to the concentration change and erratic distribution of solution, as an initial approach, a glass plate was inserted into a pure water to obtain the glass position and its thickness. There, the interesting result was observed, that is, the vibration mitigating waveform like a diffraction pattern by a knife-edge was observed. The OCT measurement consists of inline signals from the back-reflected (scattered) light, while the diffraction pattern by a knife-edge is appeared on a screen. This phenomenon causes the boundary burr on the target detection, while the diffraction pattern has the information of the refractive index difference of the target. We shift the experiment to more simple arrangement to examine this unique phenomenon. With the actual knife-edge diffraction conditions, we discussed the boundary burr phenomenon of the OCT signal. The numerical analysis approach was started, too.

In this report, the characteristics of the boundary burr phenomenon is examined and analyzed. Its origin is considered experimentally and analytically. The influence and benefit of this boundary burr phenomenon was discussed, too.

[a] https://orcid.org/0000-0001-9292-4523

115

2 LONG-PATH TD-OCT SYSTEM

The time-domain OCT is classical and scanning speed is lower than the current trend Spectral Domain OCT, but it has a simple structure and linear signal magnification, and higher flexibility of optical probe design independent to the other OCT specification such as scan speed, wavelength and scanning range.

The optical setup of the long path TD-OCT is illustrated in Fig.1. The SLD (Super Luminescent Diode) light source of 800nm-band is installed into the long path TD-OCT. The cylindrical can-package designed original SLD has been developed for our industrial OCT. Peltier device for cooler was excluded in this SLD device to keep the cheaper cost. Even without a cooler, its optical intensity and operation are stable for industrial use. It is produced by Anritsu Co, Ltd. The interference signal is detected as the Gaussian envelope through the specialized amplifier and filter circuit.

The long path TD-OCT utilizes the rotational optical path change mechanism. (Shiina, 2002) This scanning mechanism consists of a rotating corner reflector and a fixed mirror. The rotation radius and its speed decide the measurement range and scan rate, respectively. The fixed mirror reflects the thrown beam to the same path. The optical path change becomes approximately linear motion. The distortion is about 1 – 2% within the rotation angle of +/-20 degrees. It causes the beat frequency change, too, as shown in Fig.2. The long-path OCT has a rotation disk of 60mm radius, of which maximum measurement range reaches 100mm. Here it is restricted to 80mm by the reflector size. The rotation speed is 200rpm. A servo motor is installed to stabilize the rotation. The rotation disk has a ballast weight to keep a valanced rotation. Even that, the rotation sometimes fluctuates slightly as a rotation jitter due to the timing of the excitation control. The interference signal was examined via a PC automatic measurement program. Such a fluctuated signal was trimmed away and took an average to minimize the standard deviation by the program. As a result, the total error restricted within 1μm.

In the last time, the OCT measurement probe was set to enter the small tank within the measurement range. The interference signals of the small tank were obtained at four positions from its glass walls (each side of the walls). The refractive index was calculated by the optical path length between the inner water sides of the small tank walls. The temperature was controlled to observe the change of refractive index and estimate the concentration of the solution.

The boundary burr could be observed when the additional glass plate inserted into the tank solution. This time, the experimental condition was simplified to make the boundary burr phenomenon clear compared with the usual knife-edge pattern.
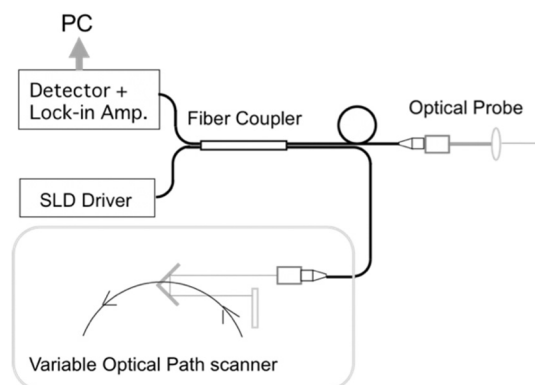

Figure 1: Structure of long path TD-OCT.

Table 1: Specification of long-path TD-OCT system.

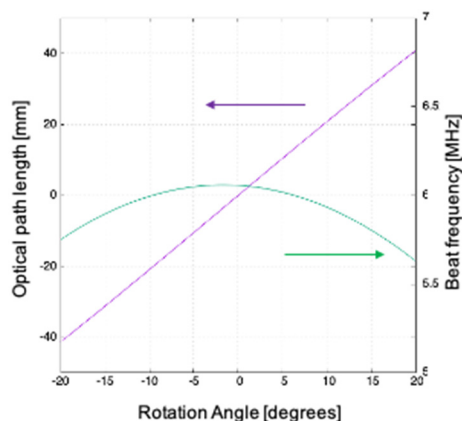| SLD	Anritsu AS8E210GP30M Center wavelength 830nm Spectral Half Width 15nm Optical Output Power 1.2mW
Fiber Assembly	2 x 2 coupler with Collimator
Scanning Mechanism	DC Servo motor with (Chiba Motor)
Rotation Disk	Diameter 120mmf Rotation Speed 200 rpm
Resolution	7μm for layer recognition 1μm for positioning accuracy
Scanning Range	100mm with +/- 20 degrees

Figure 2: Optical path length and beat frequency with optical scanning mechanism at 200rpm.

3 EXPERIMENT

To make this boundary burr phenomenon clear, the water tank was removed and put the knife-edge, for which was substituted a movable thin mirror, and the fixed mirror plate to return the light to the probe. The experimental setup is shown in Fig. 3. Figure 3(a) is the usual setup to observe the knife-edge diffraction and Figure 3(b) is this experimental setup to observe the boundary burr phenomenon with the OCT probe. In the usual knife-edge observation, the knife-edge is fixed and the diffraction pattern is appeared on the screen, which is set after the knife-edge. The distance between the knife-edge and the screen decide the diffraction pattern enlargement. On contrary, the OCT measurement is a point measurement and it catches the back reflected light. The collimator is utilized as a transmitting and receiving aperture. To obtain the pattern, the knife-edge changes its position by crossing the OCT beam.

The divergence of the optical probe beam was controlled with the adjustable collimator. The divergence was adjusted from focusing condition to spreading condition. The measurement was conducted by shifting the knife-edge mirror to be crossed the beam orthogonally. At each knife-edge mirror position, the OCT interference signal returned from the fixed mirror was stored. The diffraction like vibration mitigating waveform will be appeared in the cross-sectional graph. In the experiment, the direction crossing the beam was changed appropriately. The knife-edge position was changed during the optical probe collimator and the fixed mirror, too.

Figure 4 shows cross-sectional waveforms at each beam divergence. The horizontal axis was started with fully covered with the knife-edge mirror as initial position of "0" and when the knife-edge mirror was shifted fully from the beam, the intensity becomes constant as the right side of the graph. The interference intensity was normalized with the constant intensity.

It is clear that the boundary burr waveforms ware appeared at the beam spreading conditions. The beam focusing condition of Fig. 4(a)-(c), the propagating beam size should be smaller at the fixed mirror position, and the waveform was rising up earlier when the beam focusing becomes stronger. The beam divergence condition of Fig. 4(c)-(e), the vibration is getting stronger due to the beam divergence. Their rising up is getting earlier due to the divergence, too. In general, the distance between the knife-edge and the fixed mirror is constant, and the diffraction pattern of knife-edge never change its rising up condition at any crossing position of the knife-edge on the beam.
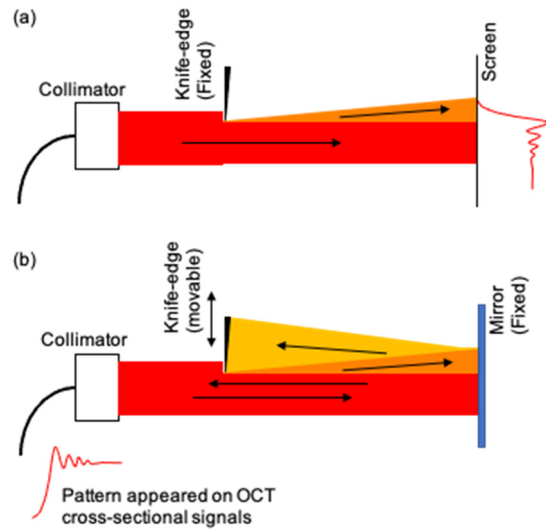

Figure 3: Experimental setup for boundary burr observation with long-path OCT.
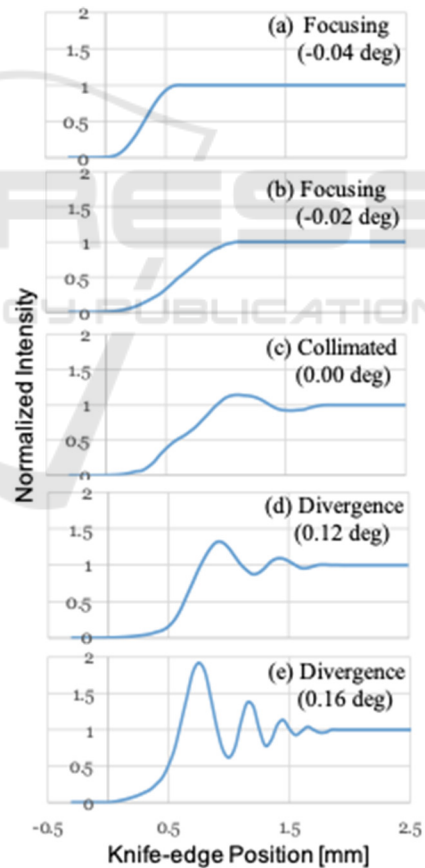

Figure 4: Observation Results due to the beam divergence.

As the rising up is getting earlier, the vibration was getting higher, while the vibration period is

getting shorter. This feature is different from the diffraction pattern of knife-edge.

Figure 5 shows the pattern difference due to the distance between the knife-edge and the collimator. The beam divergence is 0.16 degrees. This result has the same feature with the diffraction pattern of knife-edge, that is, the distance is getting longer, the pattern is enlarged and the peak intensities of the vibration is smaller. The vibration period is followed with the same manner, too.

For check, the pattern observation was conducted with both of left and right side scan of the knife-edge. The result is shown in Fig. 6. The beam divergence was 0.16 degrees. It is natural that both of the boundary burr patterns are same vibration, while we can discuss the beam size. It will burr the boundary of the target. It will be important to distinguish the time variation of the refractive index and concentration.

How this boundary burr phenomenon will occur? We considered the experimental condition with the long-path TD-OCT. Off course, it is particular condition on long-path OCT. Beam divergence will be effective on the longer optical path when it is detected on the inline collimator aperture. When the knife-edge will start from the covered position, the interference intensity rises up due to the uncovered area of the collimator aperture. Then the diffraction pattern is reflected at the fixed mirror and goes back to the collimator. At that time, as the first peak area occupies on the collimator aperture as shown in Fig. 7(i), the interference intensity rises up at maximum. The diffraction pattern of knife-edge repeats the vibration peaks equally plus and minus against the average intensity. When the knife-edge position gradually uncovers the collimator aperture area like fig. 7(ii), the interference intensity generated by the reflected beam just passed through the uncovered area will causes the vibration, too. When the number of the peaks increases, the interference intensity reaches to the average, that is, settle down to the constant (Fig. 7(iii)). The distance R between the knife-edge and the collimator via the fixed mirror, wavelength λ and the adequate knife-edge position x_0 to cover the collimator aperture, that is, forming the non-unit diffraction parameter $\sqrt{\frac{2}{\lambda R}} x_0$ will decide the boundary burr phenomenon. The long-path OCT had such parameters balance and observed those patterns.
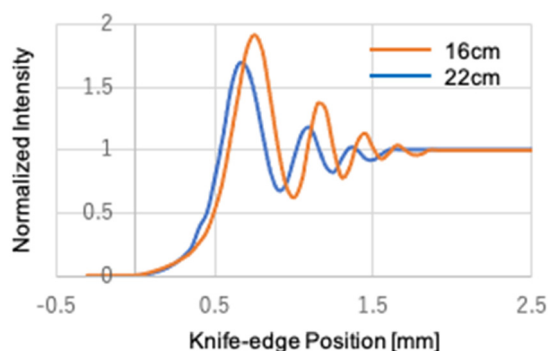

Figure 5: Pattern variation due to the distance between the knife-edge and the fixed mirror. The beam divergence is 0.16 degrees.
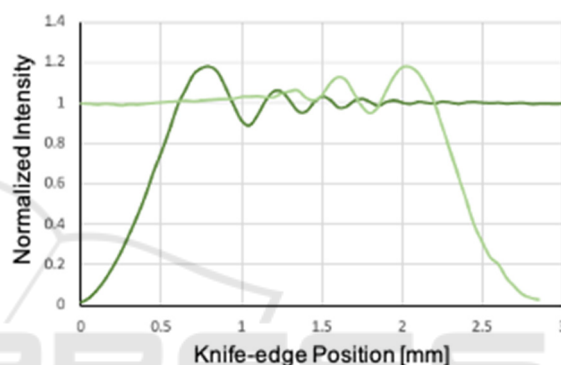

Figure 6: Left and right sides boundary burr patterns. The distance between the knife-edge and the collimator was 22cm.
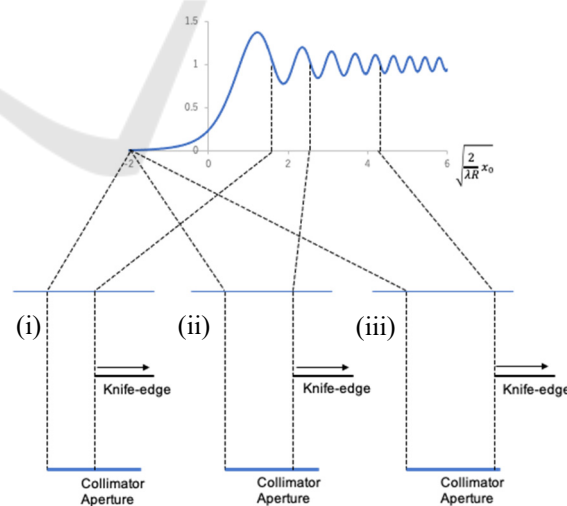

Figure 7: Principle of boundary burr phenomenon on long-path OCT observation.

4 SIMULATION

To make this boundary burr phenomenon clear, we conducted the numerical simulation. The experimental condition is considered in the simulation, for example, wavelength, knife-edge setup, propagation distance, aperture size, etc. The diffracted beam propagates to a certain distance. This diffracting intensity distribution is visualized. We set the orbicular beam and the orbicular collimator aperture, and calculate the 2 dimensional intensity distribution. The Gaussian distribution was used in the calculation. Larger the intensity to renter into the aperture is, Stronger the interreference intensity is. The parameters are propagation distance between the knife-edge and the collimator via the fixed mirror. The core size of the optical fiber was considered with the focal length of the collimator lens, too.

The intensity distribution at variation of the knife-edge position is shown in Fig.8. Each image indicates $4\mu m \times 4\mu m$ cross sectional area at the focal point of the collimator. The center circle indicates the core area, which estimates the intensity passed through the core. The back arrow with a line represents the shadow of the knife-edge, that is, the knife-edge inserted from the left side. Its position is shown in the unit of radius R. The distance between the knife-edge and the collimator via the fixed mirror was adjusted to reflect the experimental condition.

When the knife-edge is placed at the position of 0.5R, where 3/4 area was covered. Although 1/4 of the aperture area is still remained, the intensity will not rise up. The peak intensity is clear, while it shifts outside from the knife-edge position. From the knife-edge position of 0.25R, the returned beam could pass through the collimator. When the knife-edge position of -0.25R, the vibration of intensity was started.

Figure 9 shows the intensity distribution due to the knife-edge position. The same boundary burr pattern can be simulated, while the concrete matching is not discussed with intensity ratio and knife-edge positions. Nevertheless, the feature of the pattern reflects the phenomenon. The intensity rises up when the reflected beam passes through more than 1/4 area of the aperture. The intensity peak was obtained at 0.25R, where the peak intensity in the distribution reach at the center. After that, the small vibration still remained but soon settle down to the average. The rising up period is matched with the experimental result. The vibration period looks similar to the experiment, but the second peak is small. The pattern variation was discussed with the change of beam divergence and the combination of the collimator lens focal length and the core size of the optical fiber.
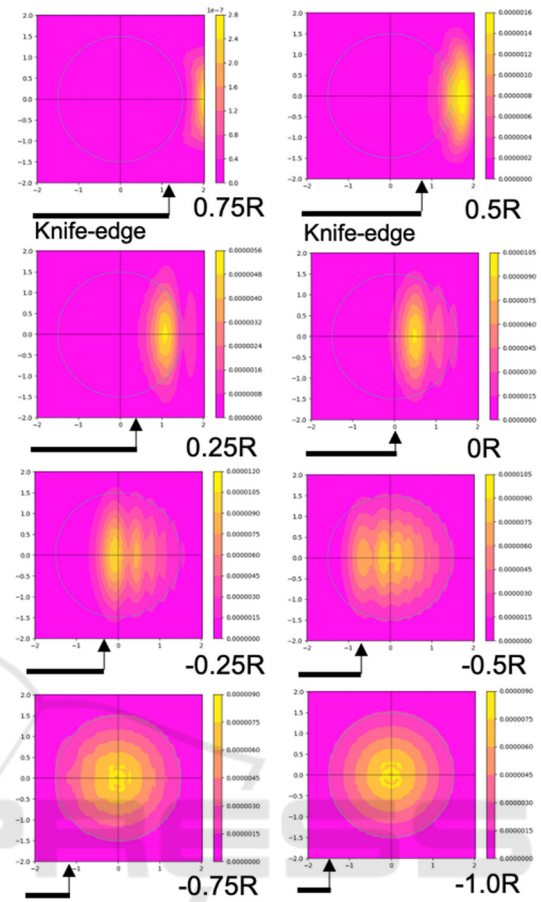

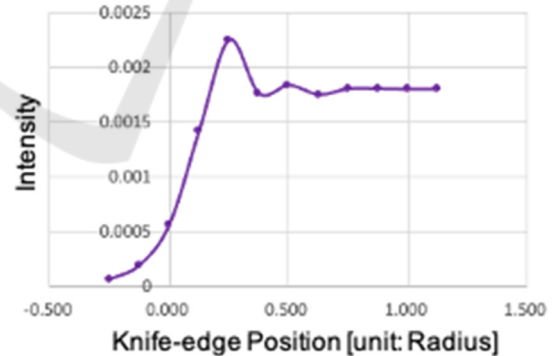Figure 8: Intensity distributions at each knife-edge position.

Figure 9: Intensity distribution of simulated result.

5 DISCUSSIONS

As the result of this experiment, for sensing purpose, when the target in the media tank will be detected, its size and boundary will be burr with this experimental condition. Such situation is depicted in Fig. 10(a). In such a case, the beam can be focused to avoid the
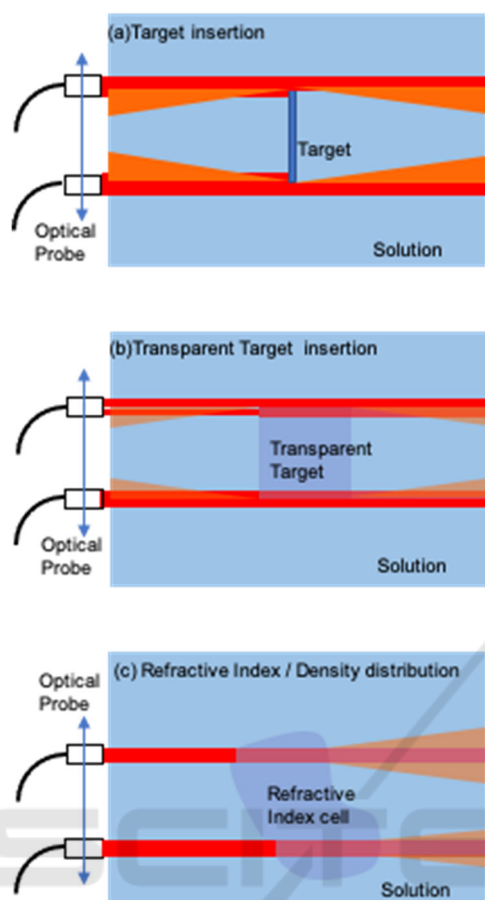
Figure 10: Step up procedure of the experiment.

boundary burr phenomenon. The focused beam, however, change the resolution, especially it should be careful in the long-path measurement. The boundary burr phenomenon is not only observed at the fixed mirror, but also at the target reflected signal itself. It is caused by the propagation of the target reflected signal to the collimator. It is observed at the experimental result (Shiina, 2020).

The boundary burr pattern has the information of the optical property conditions such as refractive index, target hitting angle, at so on. The known material target is inserted into the solution to reveal the phenomenon about the combination of target material and the solution as shown in Fig.10(b). The refractive index of the target will change the diffraction condition. It is helpful to tie up with the numerical analysis with the theory.

The goal of this project is to visualize the distribution of the refractive index and concentration of the target solution as shown in Fig.10(c). They change due to the temperature and chemical reaction. The boundary burr pattern reflects them. The

sensitivity and resolution is quite high, and this system can catch the small difference of the ignition of change such as freezing reaction and convective flow, and so on.

6 CONCLUSIONS

In this report, we have developed the long-path TD-OCT with the positioning accuracy of 1μm and measurement range of >80mm. With this experimental set up, the vibration mitigating waveform like a diffraction pattern by a knife-edge was observed. The boundary burr phenomenon is caused by the propagation of the diffraction pattern. It is proved experimentally and analytically.

The goal of this project is to visualize the distribution of the refractive index and concentration of the target solution. Now the experiment shifts to the next step, that is, the target is inserted into the solution to obtain its distribution with the information of refractive index, position and concentration change due to the temperature and chemical reaction.

REFERENCES

Brezinski M. E. and Fujimoto J. G., 1999, "Optical Coherence Tomography: High-Resolution Imaging in Nontransparent Tissue", IEEE J. Quant. Electron., Vol. 5, No. 4, pp.1185-1192.

Danielson B. L. and Boisrobert C. Y. 1991, "Absolute optical ranging using low coherence interferometry", App. Opt. Vol. 30, No.21 pp.2975-2979.

Harvey A. H., Gallagher J. S., and J. M. H. L., 1998, "Revised Formulation for the Refractive Index of Water and Steam as a Function of Wavelength, Temperature and Density", J. Phys. Chem. Ref. Data, Vol.27, pp.761-774.

Huang D., Swanson E. A., Lin C. P., Schuman J. S., Stinson W. G., Chang W., Hee M. R., Flotte T., Gregory K., Puliafito C. A., J. G. Fujimoto, 1991, "Optical Coherence Tomography", Science, Vol. 254, pp.1178- 1181.

Saeki K., Huyan D., Sawada M., Sun Y., Nakamura A., Kimura M., Kubota S., Uno K., Ohnuma K., and Shiina T., 2020, "Measurement algorithm for real front and back curved surfaces of contact lenses", Applied Optics, Vol. 59, No. 28, pp.9051-9059.

Shiina T., Moritani Y ., Ito M., and Okamura Y ., 2003, "Long optical path scanning mechanism for optical coherence tomography", Applied Optics, Vol.42, No. 19, pp.3795-3799.

Shiina T., Miyazaki H., and Honda T., 2009, "Factory built-in type simplified OCT system for industrial

application", IEEJ C、Vol.129, No.7, pp.1276-1281, (Japanese)

Shiina T., 2014, "Optical Coherence Tomography for industrial application" Handbook of Optical Metrology 2nd Edition, CRC Press, Chapter 30, pp.769 – 790.

Shiina T. 2019, "Solution Concentration and Temperature Measurements by Long-path Optical Coherence Tomography", Photoptics 2020, 20-RP-33.

Song G. and Harding K G, 2012, "OCT for industrial applications", *Proc. Of SPIE*, 8536.

Tanno N. 1990, Japanese Patent 2010042.

Yoshizawa t. Eds, 2015, *Handbook of optical metrology: principles and applications, second edition,* CRC Press.